UDK 669.017.12:621.7.019
Original scientific article/Izvirni znanstveni članek

ISSN 1580-2949
Mater. Tehnol.

MICRO VICKERS HARDNESS AND SURFACE ROUGHNESS OF Al-Cu UNS A92124/T851 ALLOY IN RELATION TO TURNING PARAMETERS: AN EXPERIMENTAL STUDY

MIKROTRDOTA PO VICKERSU IN POVRŠINSKA HRAPAVOST Al-Cu ZLITINE UNS A92124/T851 V ODVISNOSTI OD PARAMETROV CNC STRUŽENJA; EKSPERIMENTALNA ŠTUDIJA

S. Vellingiri[1*], G. Sundara Vadivel[2*], A. Arunkumar[3], S. Sivamani[4]

[1*]Department of Mechanical Engineering, Coimbatore Institute of Technology, Coimbatore, Tamil Nadu, India, 0000-0002-1273-738X
[2*]Department of Mechanical Engineering, E.G.S. Pillay Engineering College, Nagapattinam, Tamil Nadu, India, 0009-0002-9021-3116
[3]Department of Mechanical Engineering, E.G.S. Pillay Engineering College, Nagapattinam, Tamil Nadu, India, 0000-0003-4060-0337
[4]Department of Electrical and Electronics Engineering, E.G.S. Pillay Engineering College, Nagapattinam, Tamil Nadu, India, 0000-0002-6627-4712
*These authors contributed equally (co-second authors)

Prejem rokopisa – received: 2025-06-29; sprejem za objavo – accepted for publication: 2026-03-21

doi:10.17222/mit.2025.1510

This study examines the effect of cutting speed and feed rate on the surface roughness and microhardness of UNS A92124-785 during CNC turning. The machined surfaces were evaluated in terms of surface roughness, microhardness, and corrosion behavior, while surface morphology and elemental characteristics were analyzed using SEM coupled with EDX. The results indicated that surface roughness (Rz) increased mainly with feed rate and showed moderate dependence on cutting velocity, with further deterioration observed after corrosion due to increased surface irregularities. Microhardness measurements revealed minimal variation with machining parameters before corrosion. However, a noticeable reduction in Vickers microhardness (VH) was observed after corrosion, suggesting surface softening. Overall, the findings highlight feed rate as the dominant factor influencing surface quality and demonstrate that corrosion adversely affects both surface integrity and hardness of the machined material.

Keywords: Vickers microhardness, surface roughness, UNS A92124/T851, cutting speed, feed rate

V članku avtorji opisujejo študijo vpliva hitrosti rezanja in pomika na hrapavost površine ter mikrotrdoto obdelovanca iz Al-Cu zlitine tipa UNS A92124-785, nastali kot posledica mehanske CNC obdelave s struženjem. Avtorji so po struženju ocenili hrapavost površine, mikrotrdoto in njeno korozijsko obnašanje. Morfologijo površine in elementarne značilnosti pa so analizirali z vrstičnim elektronskim mikroskopom (SEM) v povezavi z spektroskopijo disperzije rentgenskih žarkov (EDX). Rezultati so pokazali, da se je hrapavost površine (Rz) povečevala predvsem s hitrostjo pomika in zmerno tudi v odvisnosti od hitrosti rezanja. Pri tem je bilo po koroziji opaženo nadaljnje poslabšanje zaradi povečanih površinskih nepravilnosti. Meritve mikrotrdote so pokazale minimalne spremembe v parametrih obdelave pred korozijo. Vendar pa je bilo po koroziji opaženo opazno zmanjšanje mikrotrdote po Vickersu (VHN), kar kaže na mehčanje površine. Na splošno ugotovitve študije poudarjajo hitrost pomika kot prevladujoči dejavnik, ki vpliva na kakovost površine. Korozija dodatno negativno vpliva tako na celovitost površine kot na trdoto obdelanega materiala.

Ključne besede: mikrotrdota po Vickersu, hrapavost površine, Al-Cu zlitina tipa UNS A92124/T851, hitrost rezanja, hitrost pomika

1 INTRODUCTION

Al–Cu alloys are extensively used in aerospace, automotive, and structural engineering applications due to their high strength-to-weight ratio, good fatigue resistance, and favorable machinability. Among them, UNS A92124/T851 alloy is particularly valued for its enhanced mechanical strength obtained through solution heat treatment and artificial aging. However, the performance and service life of components manufactured from this alloy are strongly influenced by the quality of the machined surface, particularly when used in load-bearing or corrosive environments.

In machining operations, such as CNC turning, process parameters, including cutting speed and input rate, play a critical role in determining surface integrity. Surface roughness is a key indicator of machining quality, as it directly impacts fatigue strength, wear resistance, corrosion behavior, and dimensional accuracy. Similarly, Vickers microhardness reflects near-surface mechanical properties, which can be altered due to plastic deformation, strain hardening, or thermal effects generated during cutting. Therefore, grasping the relationship between turning parameters and both surface roughness and microhardness is essential for optimizing machining performance.

*Corresponding author's e-mail:
giriarunvellingiri@gmail.com (S. Vellingiri)

A previous study reported that cutting speed and feed rate were identified as the most influential parameters affecting tool wear and surface roughness in the micro-turning of a titanium alloy. Optimal performance was achieved at 3035 min^{-1}, 7.5 µm/rev feed, and 15 µm depth of cut, resulting in 0.149 mm tool wear, 0.691 µm surface roughness, and 89 % desirability.[1] The hybrid RF-Reg and MO-GWO framework successfully optimized SLM parameters, achieving 98.63 % relative density, 236.60 HV microhardness, and 23.42 µm surface roughness at 197.93 W laser power, 753.40 mm/s scanning speed, and 0.05 mm hatch spacing, with minimal experimental error. The optimized CuFeMnNi HEA exhibited superior mechanical, wear, and corrosion performance, confirming the effectiveness of the proposed multi-objective optimization approach.[2]

Response surface methodology using a Box–Behnken design successfully modelled the effects of nozzle distance, pressure, impact angle, and exposure time on microhardness and residual stress of 2124-T851 aluminum alloy. Multi-response optimization through the desirability function identified optimal peening conditions, which were experimentally validated by hardness, residual stress, XRD, surface morphology, and roughness analyses.[3] Numerical and experimental investigations revealed that increasing surface roughness reduces the group velocity of A0 and S0 modes and alters their amplitudes, significantly affecting LUGW propagation characteristics. Experimental validation using T-SAFT imaging confirmed that higher roughness (0.61–3.82 µm) decreases A0 mode velocity and amplitude, thereby reducing defect detection and localization accuracy.[4] Sandblasting significantly influenced the surface characteristics and corrosion behaviour of SS400 mild steel, with steel grit producing the highest surface roughness (62.08 µm) and silica sand yielding the lowest corrosion rate (0.0000175 mm/year). The results indicate that abrasive selection should balance roughness and electrochemical performance. Steel grit is preferable for improved coating adhesion, while silica sand is more suitable for minimizing corrosion in railway maintenance applications.[5]

Nanostructured sol–gel silica–zirconia coatings synthesized via dip-coating effectively enhanced the corrosion resistance of AA2024-T3 aluminum by limiting electrolyte diffusion and oxygen access to the substrate. Electrochemical impedance, surface morphology, roughness, and microhardness analyses confirmed that optimized annealing conditions improved coating stability and demonstrated strong potential for marine anti-corrosive applications.[6] RSM and ANOVA analysis revealed that spindle speed, depth of cut, and feed rate significantly influence surface roughness, cutting force, and chip characteristics during Ti6Al4V turning, with regression models accurately predicting performance. The ANFIS-based offline digital twin, validated through additional experiments, identified optimal parameters (656.52 min^{-1}, 0.3 mm DoC, 30 mm/min feed), demonstrating an effective predictive framework for surface quality control and productivity enhancement.[7] Incorporation of nano-MoS_2 particles in the MQL environment significantly improved machining performance during AA2024 turning, achieving a minimum surface roughness of 0.8399 µm and tool wear of 0.024 mm at optimized cutting conditions, with a 28 % reduction in Ra compared to dry cutting. Machine learning models effectively predicted surface roughness, with Gradient Boosting and Linear Regression demonstrating superior accuracy (R^2 = 1.000 and 0.999), confirming the reliability of the predictive framework.[8] Taguchi L27 analysis revealed that discharge current is the most influential parameter affecting MRR, TWR, and surface roughness in EDM of AISI D2 steel, with higher current and pulse-on time significantly improving MRR but increasing tool wear and surface roughness. Optimal balanced performance was achieved at 5 A discharge current, 150 µs pulse-on time, and 40 µs pulse-off time, yielding improved surface quality (3.5 µm SR) with controlled tool wear and productivity.[9]

Friction stir welding of 304 SS and 2024-T3 Al alloy produced a wavy interface with embedded steel fragments and thin IMCs, leading to significant microstructure-driven improvements in performance. The FSWed joint exhibited superior corrosion resistance and wear performance, with lower corrosion rate, wear rate, surface roughness, and wear depth compared to the base 2024-T3 alloy.[10] Another study demonstrated that thermal conductivity and hardness significantly influence surface integrity during CNC turning, with higher thermal conductivity materials generally producing lower surface roughness and reduced variability. Validated probabilistic models ($R^2 > 0.95$) confirmed strong predictive capability, enabling material-specific optimization of machining parameters to improve surface quality, tool life, and component reliability.[11] Another study revealed that increasing cutting speed and feed rate during CNC turning of Cu–Al–Mn shape memory alloys enhances material removal rate but also increases cutting force, while higher Mn content significantly improves machinability. CAM 3 demonstrated superior performance with up to 88 % higher MRR, lower cutting forces, 42 % reduced surface roughness, and smoother chip morphology compared to CAM 1, confirming the beneficial role of manganese in improving machining efficiency and surface quality.[12]

A study optimized CNC turning of 7075 aluminum alloy using Taguchi, Grey Relational Analysis, and Desirability Function Analysis to simultaneously minimize surface roughness and maximize MRR, achieving a highly predictive model (R^2 = 90.23 %). Tool type was the most influential parameter (44 % overall; 63 % for Ra), and the optimized conditions (175 m/min, 0.05 mm/rev, 0.1 mm depth) were predicted to achieve a minimum surface roughness of 0.416 µm.[13] Another study investigated the influence of cutting parameters on surface finish during dry flank milling of Aluminum 6061 using HSS tools, employing ANOVA and second-order regression modelling to analyze transverse and longitudinal surface quality. The developed predictive models effectively describe parameter–surface relationships, enabling reduced machining errors and improved product quality.[14] A study evaluated the machining performance of AA2024-T351 under dry, MQL, LN_2, and CO_2 cooling using advanced measurement techniques for tool wear, surface roughness, power consumption, and microhardness. Results confirmed that cryogenic cooling significantly enhances machining characteristics, with CO_2 and LN_2 reducing surface roughness by up to 39.28 % and power consumption by up to 11.5 % compared to dry conditions.[15] Another study developed a sustainable AA3105-based MMC reinforced with eggshell ash and iron slag using $MgSO_4$ as a chemical aid, achieving improved particle dispersion and grain refinement up to 10 *w*/% reinforcement. The optimized composite showed ≈30 % increase in hardness with acceptable surface roughness (≤20 % rise in Ra), demonstrating the feasibility of waste-derived reinforcements for eco-friendly structural applications[16]. A reference study investigated the influence of aging time, temperature, and applied stress on the creep aging behavior of 2124 aluminum alloy, revealing that creep strain and rate increase with higher process parameters, while hardness follows a low–peak–low trend. Optimal mechanical properties were achieved at 200 MPa, 185 °C, and 8 h due to the coexistence of strengthening S' phases, with TEM confirming a stress-assisted precipitate formation without significant orientation effects.[17]

Another study evaluated the effect of copper content and cutting parameters on the microstructure, hardness, and machinability of sand-cast Al–Cu alloys under MQL conditions, showing that hardness and cutting forces increase with Cu addition, with Al-8Cu exhibiting the highest hardness (95 HB) and cutting force (216.03 N). Statistical analyses (ANOVA and regression) identified cutting velocity as the most influential factor for cutting and feed forces, followed by material type and feed rate, while SEM/EDS confirmed flank wear and aluminum adhesion on tools.[18] Another study fabricated AA2024–TiO_2 nanocomposites (0–7.5 *w*/%) via stir casting and examined their microstructure and mechanical properties using SEM, EDS, XRD, tensile, and hardness tests. An addition of 7.5 *w*/% TiO_2 improved ultimate tensile strength by 37 % and elongation by 71 % but reduced hardness by 14 %, while maximum hardness was achieved at 5 *w*/% TiO_2 reinforcement.[19] Another study investigated the tensile behavior of Mg-1Sn-1Ca and Mg-2Sn-0.5Ca alloys and the influence of resistance spot welding parameters on joint microstructure and strength. Microstructural and hardness analyses revealed that optimized conditions (0.6 kN, 0.4 s, 16 kA) yielded a maximum joint strength of 1.001 kN, providing guidance for improving magnesium alloy welding performance.[20]

1.1 Novelty

Previous studies on Al–Cu alloys reported that feed rate generally has a dominant influence on surface roughness, while cutting speed may impact tool–workpiece interaction, temperature distribution, and subsurface microstructural changes. However, limited experimental data are available specifically for UNS A92124/T851 alloy regarding the combined evaluation of surface roughness and Vickers microhardness under varying turning conditions.

1.2 Present research

This study focused on experimentally investigating the effect of cutting speed and feed rate on the surface roughness and Vickers microhardness of Al–Cu UNS A92124/T851 alloy during CNC turning. The objective was to identify optimal machining conditions that ensure improved surface integrity and mechanical performance, thereby supporting its application in high-performance engineering components.

2 MATERIALS AND METHODS

2.1 Al-Cu UNS A92124/T851 alloy

Al-Cu UNS A92124/T851 alloy, commonly known as Aluminum 2124-T85, together with its chemical composition, its mechanical and thermal properties is presented in the table below. The alloy exhibits superior strength and fracture toughness and is primarily used in aerospace applications. **Table 1** shows the composition, as well as mechanical, and thermal properties of the alloy determined by arc atomic emission spectroscopy (AES).

Table 1: Al-Cu alloy UNS A92124/T851 composition (*w*/%) and properties

Composition (*w*/%)							
Cu	Mg	Mn	Fe	Zn	Si	Ti	Al
4.9	1.8	0.9	0.3	0.25	0.2	0.15	Remaining
Mechanical properties			Thermal properties				
Elastic modulus	71 GPa		Thermal conductivity	150 W/m-K			
Poisson's ratio	0.33		Thermal expansion	23 μm/m-K			
Tensile strength	490 MPa		Specific heat capacity	880 J/kg-K			
Shear strength	280 MPa		Melting point	640 °C			

2.2 CNC turning

A M08SY turning center was used for CNC turning operations involving Al-Cu UNS A92124/T851 alloy. **Figures 1** and **2** show the dimensions of the workpiece and the turning process. **Table 2** lists the experimental machining parameters for the turning operation, which were a constant depth of cut of 1.2 mm, a cutting velocity range of 30–90 m/min, and a feed rate range of 0.04–0.20 mm/rev.

Table 2: Experimental machining conditions

Depth of cut, mm	Cutting velocity, m/min	Feed rate, mm/rev
1.2	30 50 70 90	0.04 0.08 0.12 0.16 0.20

2.3 Surface roughness measurement

Al-Cu UNS A92124/T851 alloy's machined surface roughness characteristics were examined using a Taylor-Hobson Talysurf tester with ASTMB117. The primary roughness characteristics under the given operating conditions were determined by analyzing the Ra and Rz parameters of the machined surface. The machined surface's roughness is seen in **Figure 3**. Equations (1) and (2) employed maximum profile height (Rz) and average roughness (Ra) as the characteristics for estimating surface quality.

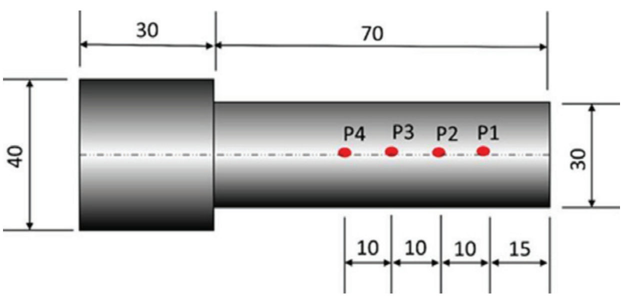

Figure 1: Sample geometry of Al-Cu UNS A92124/T851 alloy with positions for hardness testing indentation

Figure 2: CNC turning center

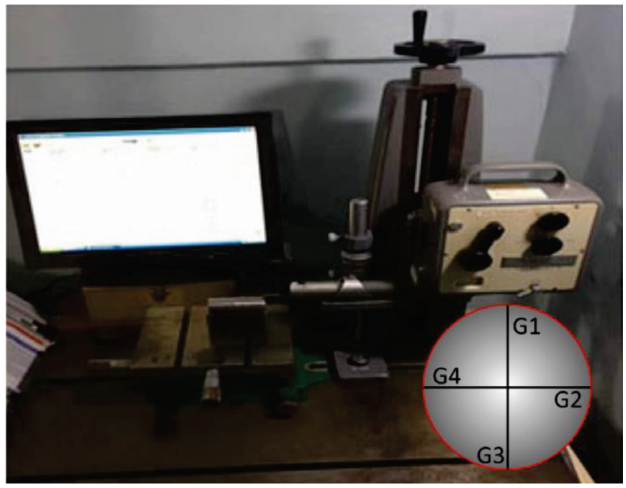

Figure 3: Surface roughness tester setup (Taylor Hobson Talysurf)

$$Ra = \frac{1}{ls}\int_{0}^{ls} |H(x)| \mathrm{d}x \tag{1}$$

$$Rz = Hp + Hv \tag{2}$$

$H(x)$ is the height of the profile, ls is the sampling length, Hp is the peak height, and Hv is the roughness profile's peak-to-valley height.

2.4 Vickers microhardness measurement

Microhardness measurements were carried out on both machined and unmachined surfaces of the Al–Cu UNS A92124-T851 alloy in accordance with ASTM E92-17 standard procedures. The test was performed at four different locations (P1, P2, P3, and P4) as illustrated in **Figure 1**. A load of 0.5 N was applied using a Vickers indenter with a square-based pyramidal geometry and an included angle of 136° between opposite faces. All measurements were conducted at room temperature, and the average hardness value was obtained from multiple indentations to ensure repeatability and accuracy.

2.5 Corrosion testing

According to the ASTM G36 standard, corrosion experiments were performed using chemical measurements. Three rectangular sections of the Al-Cu UNS A92124/T851 alloy with dimensions of (5 × 5 × 6) mm were used. Each piece was cleaned with emery paper of grades 200–800 to produce a mirror finish before the experiment. A 2.0 N hydrochloric acid (HCl) solution was prepared using doubly distilled water. In this technique, the metal pieces were immersed in beakers containing 50 mL of 2.0 N HCl for 72 h at room temperature. Before immersion, each item was weighed. Using the weight-loss method, corrosion rates of the metals were calculated based on their area, density and immersion time.

2.6 Microstructure examination

The microstructure and elemental composition of the machined and unmachined Al–Cu UNS A92124-T851 alloy were investigated using scanning electron microscopy (SEM) coupled with energy dispersive X-ray (EDX) analysis. Before examination, the specimens were metallographically prepared through standard grinding and polishing, followed by chemical etching to reveal the surface morphology. Microstructural features were examined at appropriate magnifications to analyze grain morphology and phase distribution. The average grain size was determined in accordance with the ASTM E112 standard using the standard grain-size Equations (3–5).

$$N = 2(A^{-1}) \tag{3}$$

$$n = n_{\text{A}} + K \tag{4}$$

$$K = 2\lg_2\left(\frac{\mu}{100}\right) \tag{5}$$

Here, N is the number of grains, n is the size of the grain, n_A is the size of the visible grain, K is the correction factor, and μ is the micrograph magnification.

3 DISCUSSIONS

3.1 Effects of cutting velocity and feed rate on Ra and Rz

It was found that the most influential surface roughness predictor was feeding. A general tendency to increase with f was shown by both Ra and Rz, independent of v_c. For f values of 0.04–0.20 mm/rev, the trend is more evident. Higher surface roughness was found, influenced by the corresponding corrosion rate in the sample at a feed rate of 0.10 mm/rev. The effect of f was amplified by up to four times at 0.20 mm/rev for post-corrosion samples compared with 0.1 mm/rev. In a low f range (0.04–0.20 mm/rev), the effect of the feed rate was less apparent. With low f values, Ra and Rz demonstrated values identical to those for the samples before machining. When v_c was changed, no major variations in Ra or Rz were observed. Consequently, the influence of feed-induced natural roughness was prevalent.

Changes in cutting speed can have thermal effects in machining operations due to the formation of a built-up edge (BUE), which can modify the consistency of the surface. The wear of this secondary adhesion layer is generally a function of severe thermo-mechanical feed effects during dry machining of this alloy. For low feed rates, however, the cutting speed effect becomes more significant, resulting in higher BUE at higher cutting speeds. The low cutting speed used in this study, however, made this effect less noticeable, resulting in almost negligible effects of the cutting speed on surface roughness. It should be remembered that all these results are in strong alignment with previous studies reporting on the parametric analysis of surface roughness in 2000- and 7000-series aluminum alloys.

In the corrosion process, no major changes in Ra were observed. However, the dispersion in the data tended to be slightly higher. This was more evident for Rz. Given that Ra was defined as the mean value of the peaks and valleys of the roughness profile, these results can be explained, whereas Rz was calculated as the maximum profile height. The pitting and intergranular corrosion phenomena are the result of surface irregularities, which may have influenced microgeometric deviation at one point, especially in the intermetallic components (Al 23 CuFe 4), **Figure 6**. Additionally, after the corrosion process, a rise in Rz, regardless of v_c and f, was ob-

Table 3: Values of surface roughness (Ra) for different input parameters before and after the corrosion phase

Ra (µm)	Cutting velocity, Vc (m/min)									
	Before corrosion					After corrosion				
Feed, f (mm/rev)	30	50	70	90	unmachined	30	50	70	90	unmachined
0.04	0.39	0.39	0.39	0.39	0.38	0.41	0.41	0.41	0.41	0.41
0.08	0.45	0.41	0.47	0.5	0.38	0.47	0.43	0.5	0.52	0.41
0.12	0.52	0.61	0.59	0.55	0.38	0.55	0.63	0.62	0.57	0.41
0.16	0.89	0.92	1.21	1.1	0.38	0.92	0.95	1.25	1.10	0.41
0.20	1.43	1.45	1.61	1.58	0.38	1.50	1.47	1.64	1.60	0.41

Table 4: Maximum profile height (Rz) values for different input parameters before and after the corrosion phase

Rz (µm)	Cutting velocity, Vc (m/min)									
	Before corrosion					After corrosion				
Feed, f (mm/rev)	30	50	70	90	unmachined	30	50	70	90	unmachined
0.04	2.40	2.42	2.00	2.10	2.41	5.80	2.42	5.80	2.10	6.43
0.08	2.80	2.45	2.60	3.10	2.41	2.80	2.45	2.60	3.10	6.43
0.12	4.00	3.12	3.35	4.50	2.41	4.00	3.12	3.35	4.50	6.43
0.16	6.30	3.98	4.45	5.10	2.41	6.30	3.98	4.45	5.10	6.43
0.20	7.10	6.80	7.00	6.90	2.41	7.10	6.8	7.00	6.90	6.43

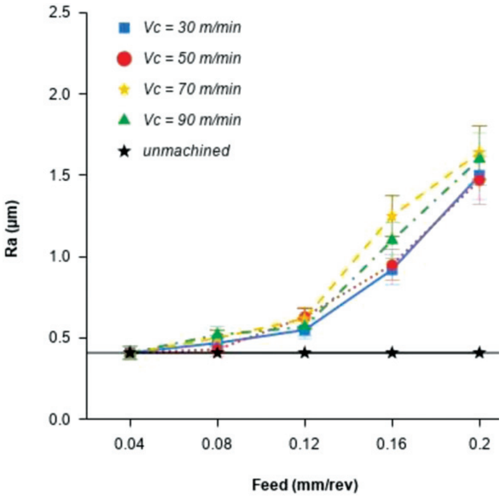

Figure 4: Before corrosion: Ra variations with feed (mm/rev) and cutting velocities (m/min)

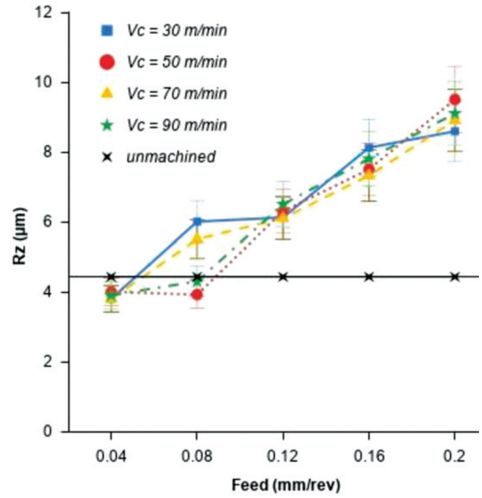

Figure 6: Before corrosion: Rz variations with feed (mm/rev) and cutting velocities (m/min)

served. In comparison with the maximum f (0.20 mm/r), this increase was just marginally larger. At elevated f values, a higher corrosion effect resulted in poor surface quality and vice versa. Consequently, only in the highest range of the values tested, the effect of f seemed to be a little higher. For different input parameters during and after the corrosion process, surface roughness (Ra) and profile height (Rz) values are shown in **Tables 3** and **4**.

3.2 Effects of cutting feed and feed rate on VHN

Figures 9 and **10** display the average microhardness values before and after corrosion for machined samples as a function of v_c and f. Moreover, the specimen's hardness values were plotted for reference. For all samples, after machining and before corrosion, an improvement in surface microhardness (HV) was commonly observed (**Figure 9**), independent of v_c and *f*. Compared to the non-machined sample, the property was improved with variation in cutting parameters, at a feed rate of 0.12 mm/rev and a cutting velocity of 50 m/min.

Figure 9 indicates smaller mean values for microhardness at v_c = 70 m/min and 90 m/min due to the cutting speed effect on microhardness, while its mean value tended to improve at v_c = 70 m/min and an intermediate f range (0.04–0.2 mm/r). Furthermore, higher dispersion was observed for this combination of cutting parameters in the experimental data. The best results for f (maximum VHN) were obtained at a feed rate of 0.16 mm/rev and a cutting velocity of 50 m/min. The VHN was 25 % different from the values obtained at other cutting velocities (50 and 90 m/min) when those values were paired with the mean v_c value (60 m/min). No clear VHN trend was observed for the other *f* values (0.12 and 0.16 mm/rev) or v_c values (70 m/min and 90 m/min). Thus, mechanical effects at low f (0.12 mm/rev) and v_c (50 m/min) values were tested using thermal effects. The

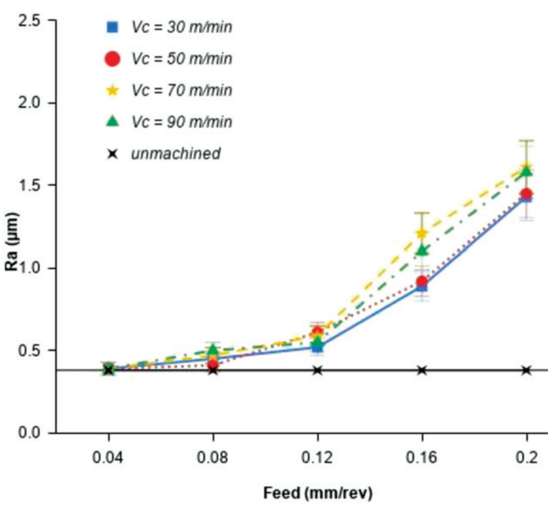

Figure 5: After corrosion: Ra variations with feed (mm/rev) and cutting velocities (m/min)

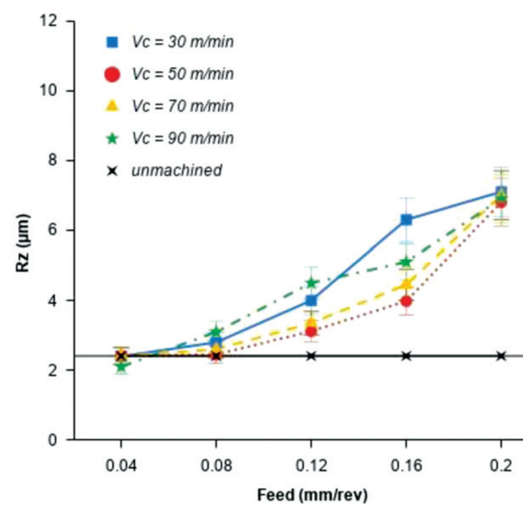

Figure 7: After corrosion: Rz variations with feed (mm/rev) and cutting velocities (m/min)

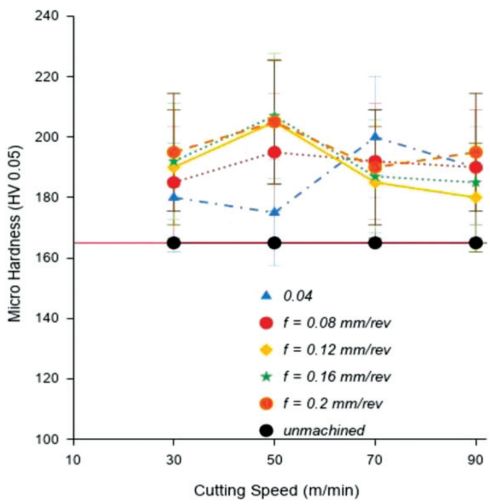

Figure 8: Before corrosion: VHN variations with feed (mm/rev) and cutting velocities (m/min)

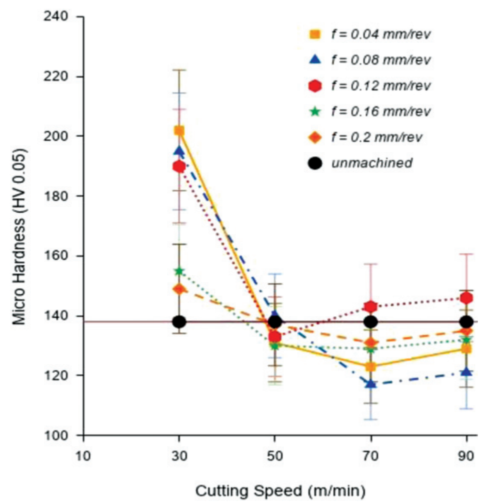

Figure 9: After corrosion: VHN variations with feed (mm/rev) and cutting velocities (m/min)

grain size was smaller than the average value of 16.75–14.55 µm.

Finally, the thermal effects were more significant at the highest cutting speed (90 m/min), while mechanical effects also played a role. The scale of grain size was therefore larger than that at low f, and the VHN was reduced to the same amount. As a consequence, mechanical and thermal effects were combined, and there was no possibility of neglecting the mechanical effects of feed within the v_c range tested against the thermal effects of cutting speed. A general decrease in the microhardness of the samples, before and after processing, was observed in VHN results following corrosion (**Figure 7**). In comparison, the range of calculated cutting parameters showed greater dispersion. The surface irregularities caused by corrosion in the tubes contributed to a strong dependency of VHN on the surface region.

Identical mean values were obtained for cutting velocities of 50 m/min and 70 m/min in the pre-machining analysis. The highest average value was obtained at v_c = 50 m/min. However, considering the high degree of dispersion indicated by the findings, it was difficult to establish a general trend. Microhardness was also adversely affected by the corrosion process; however, after corrosion, no clear relationship could be established between the machining condition, surface roughness, and Vickers microhardness. Vickers microhardness values for various input parameters before and after corrosion are shown in **Table 6**.

3.3 Microstructure examination of machined and unmachined surfaces

The SEM micrographs below (250× magnification) illustrate the surface morphology of A92124/T851 aluminum alloy before and after CNC turning. **Figure 10a** shows the unmachined surface, characterized by an irregular and heterogeneous topography with randomly distributed asperities and microvoids. The rough, uneven texture is attributed to the original rolling and heat-treatment history of the alloy, exhibiting surface undulations and microstructural discontinuities typical of wrought aluminum alloys. In contrast, **Figure 10b** presents the machined surface after CNC turning, displaying a comparatively smoother and more uniform morphology. Distinct parallel feed marks along the cutting direction are visible, indicating the tool-workpiece interaction during material removal. The reduction in surface irregularities suggests effective shearing and plastic deformation of surface asperities under controlled cutting conditions. Minor surface grooves and localized material smearing may be observed, which are typical of aluminum alloys due to their ductility and tendency for adhesion during

Table 5: VHN values for various input parameters before and after corrosion

VHN	Cutting velocity, Vc (m/min)							
	Before corrosion				After corrosion			
Feed, f (mm/rev)	30	50	70	90	30	50	70	90
0.04	180	175	200	190	202	131	123	129
0.08	185	195	192	190	195	140	117	121
0.12	190	205	185	180	190	133	143	146
0.16	192	207	187	185	155	130	129	132
0.20	195	205	190	195	149	137	131	135
unmachined	165	165	165	165	138	138	138	138

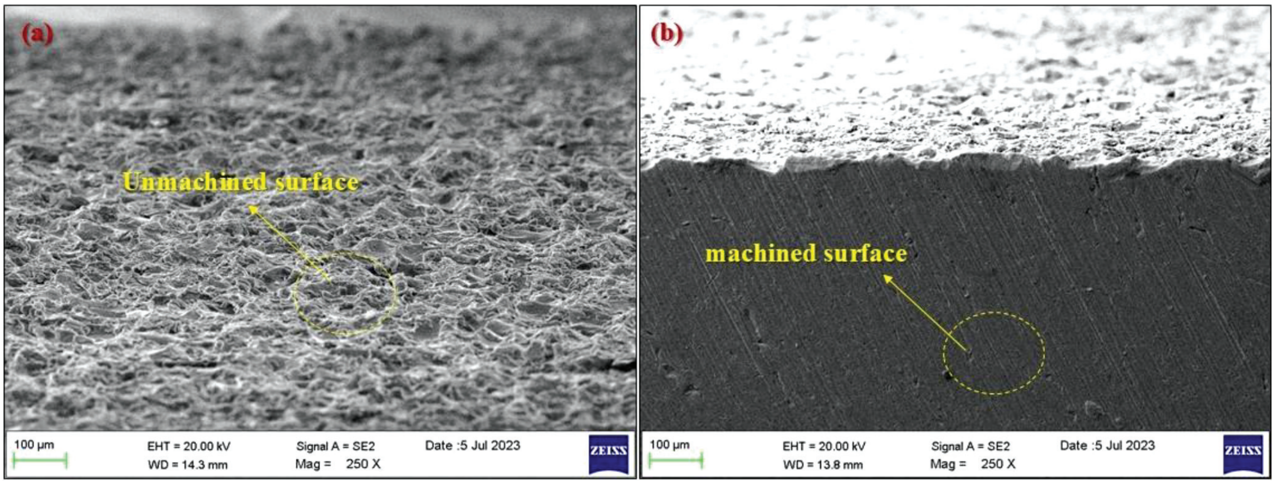

Figure 10: a) Unmachined surface and b) machined surface of Al–Cu UNS A92124-T851 alloy

machining. Overall, the machined surface demonstrates improved surface integrity and reduced roughness compared to the unmachined condition, confirming the effectiveness of the selected turning parameters in enhancing surface finish.

4 CONCLUSIONS

This study investigated the influence of cutting velocity and feed rate on the surface roughness, microhardness, and corrosion behavior of UNS A92124-785 during CNC turning. The experimental results clearly demonstrate that feed rate is the most influential machining parameter affecting surface integrity. Surface roughness parameters (Ra and Rz) increased predominantly with feed rate, while cutting velocity exhibited only a moderate effect. Higher feed rates (0.16–0.20 mm/rev) produced significantly rougher surfaces even before corrosion. After exposure to corrosion, both Ra and Rz values further increased due to enhanced surface irregularities and localized degradation, confirming deterioration of surface quality. Microhardness measurements showed relatively minor variation with machining parameters before corrosion. However, a noticeable reduction in Vickers hardness was observed after corrosion for all machining conditions, indicating surface softening and material degradation. The unmachined samples exhibited comparatively greater susceptibility to corrosion damage, reflected by a significant increase in Rz and a reduction in hardness. SEM–EDX analysis supported these findings by revealing surface morphological changes and elemental variations after corrosion exposure. Overall, the results confirm that: feed rate is the dominant factor governing surface roughness; corrosion significantly degrades surface integrity and reduces hardness; lower feed rates (0.04–0.08 mm/rev) combined with moderate cutting velocities provide improved surface quality and better resistance to corrosion-induced deterioration. Thus, careful selection of machining parameters is essential for enhancing surface performance, maintaining mechanical integrity, and improving corrosion resistance of UNS A92124-785 components.

5 REFERENCES

[1] C. Prakash, S. Selva kumar, D. Manikandan, K. Ramaswamy, Investigation of micro turning process parameters for titanium alloy using response surface methodology, Discov. Mater., 6 (**2026**) 1, doi:10.1007/s43939-025-00475-5

[2] K. Hareharen, T. Panneerselvam, Multi-objective grey wolf optimization of selective laser melting process parameters for the fabrication of Al0.2CuFeMnNi high entropy alloy and evaluation of mechanical, tribological and corrosion behaviour, Intermetallics (Barking), 186 (**2025**), doi:10.1016/j.intermet.2025.108968

[3] Y. S. Nam, Y. I. Jeong, B. C. Shin, J. H. Byun, Enhancing surface layer properties of an aircraft aluminum alloy by shot peening using response surface methodology, Mater. Des., 83 (**2015**), doi:10.1016/j.matdes.2015.06.065

[4] S. Annamalai, B. Anand Ronald, D. Ebenezer, Effect of impingement angle and impact velocity on slurry erosive wear behaviour of particulate reinforced aluminium composites, International Journal of Surface Science and Engineering, 18 (**2024**) 1, doi:10.1504/IJSURFSE.2024.136661

[5] A. Zulkarnain, F. N. S. Hardyanti, H. W. Prasetya, D. S. Atmaja, D. A. Perwira, The influence of abrasive material variations in sandblasting on surface roughness and corrosion rate of mild steel SS400, Advances in Science and Technology Research Journal, 20 (**2026**) 1, doi:10.12913/22998624/211615

[6] D. Tsamos, P. Artemiou, D. Fasnakis, D. Loizos, S. Gerardis, S. Maropoulos, Optimizing the annealing process of sol–gel hybrid coating technology for corrosion barrier protection of Al, J. Coat. Technol. Res., 23 (**2026**) 1, doi:10.1007/s11998-025-01191-8

[7] C. S. Sumesh, A. Ramesh, Developing an offline digital twin framework for predicting surface roughness in machining of Ti6Al4V alloy, Materials and Manufacturing Processes, 41 (**2026**) 1, doi:10.1080/10426914.2025.2586496

[8] R. G. Manohar, R. Rajaraman, Tribological impact and surface roughness prediction in nano-MQL assisted AA2024 machining, Proceedings of the Institution of Mechanical Engineers, Part J: Journal of Engineering Tribology, 240 (**2026**) 2, doi:10.1177/13506501251346818

[9] J. P. Agrawal, N. Somani, N. K. Gupta, Optimizing electric discharge machining parameters using Taguchi method and ANOVA: A study on AISI D2 steel machining with copper electrodes and materials

science progress, Next Materials, 10 (**2026**), doi:10.1016/j.nxmate.2025.101361

[10] F. A. Mir, N. Z. Khan, A. N. Siddiquee, S. Parvez, T. Narayana, M. H. Abidi, F. Alasim, Microstructure-driven enhancements in tribological and corrosion properties of friction stir welded Al 2024-T3/304 stainless steel joints, Tribol. Int., 211 (**2025**), doi:10.1016/j.triboint.2025.110853

[11] M. S. Alsoufi, S. A. Bawazeer, Probabilistic Analysis of Surface Integrity in CNC Turning: Influence of Thermal Conductivity and Hardness on Roughness and Waviness Distributions, Machines, 13 (**2025**) 5, doi:10.3390/machines13050385

[12] N. Praveen, N. G. S. Kumar, R. Shivashankar, C. D. Prasad, H. Soni, G. Veeresha, M. Prasad, T. C. S. Kumar, U. S. Mallik, A. A. Aden, Effect of CNC Turning Parameters on MRR, Cutting Force and Surface Roughness for Ternary Shape Memory Alloys (SMAs), Results in Engineering, 26 (**2025**), doi:10.1016/j.rineng.2025.104876

[13] I. I. Ikhries, A. F. Al-Shawabkeh, J. S. Haddad, N. A. Al-Najdawi, F. A. Alfaqs, Integrated multi-objective optimization for high-precision CNC turning of 7075 aluminum alloy, Next Materials, 9 (**2025**), doi:10.1016/j.nxmate.2025.101338

[14] A. Belamri, Y. Makhloufi, M. Methia, R. Yousfi, A. Sad Eddine, A. Benslimane, ANOVA-based analysis of cutting parameters on surface roughness in aluminum milling, International Journal of Advanced Manufacturing Technology, 139 (**2025**) 3, doi:10.1007/s00170-025-15997-8

[15] M. K. Gupta, P. Niesłony, M. Sarikaya, M. E. Korkmaz, M. Kuntoğlu, G. M. Królczyk, Studies on Geometrical Features of Tool Wear and Other Important Machining Characteristics in Sustainable Turning of Aluminium Alloys, International Journal of Precision Engineering and Manufacturing – Green Technology, 10 (**2023**) 4, doi:10.1007/s40684-023-00501-y

[16] R. Yadav, V. K. Dwivedi, S. P. Dwivedi, Implications of Eggshell Ash, Iron Slag, and MgSO4 Incorporation on the Microstructure, Microhardness, and Surface Roughness of AA3105 Sustainable Composites, Journal of The Institution of Engineers (India): Series D, (2025), doi:10.1007/s40033-025-00974-y

[17] L. H. Zhan, Y. G. Li, M. H. Huang, Effects of process parameters on mechanical properties and microstructures of creep aged 2124 aluminum alloy, Transactions of Nonferrous Metals Society of China [Internet], [accessed 2026 Mar 1], 24 (**2014**) 7, 2232–2238, doi:10.1016/S1003-6326(14)63338-0

[18] F. Ficici, I. Ozdemir, T. Grund, T. Lampke, Investigation of the effect of copper content added to aluminum on cutting force in MQL turning, Sci. Rep., 16 (**2026**) 1, doi:10.1038/s41598-025-34458-6

[19] H. M. Mahan, S. V. Konovalov, K. Osintsev, I. Panchenko, The Influence of TiO_2 Nanoparticles on the Mechanical Properties and Microstructure of AA2024 Aluminum Alloy, Materials and Technology, 57 (**2023**) 4, doi:10.17222/mit.2023.898

[20] W. Hou, Z. Jia, Q. Chen, X. Niu, Research on the Microstructure and Mechanical Properties of Dissimilar Magnesium Alloys Using the Resistance Spot Welding Method, Materials and Technology, 59 (**2025**) 4, doi:10.17222/mit.2025.1399